Asia-Pac. J. Atmos. Sci., 53(2), 273-285, 2017
DOI:10.1007/s13143-017-0030-7

pISSN 1976-7633 / eISSN 1976-7951

Combined Effect of the East Atlantic/West Russia and Western Pacific Teleconnections on the East Asian Winter Monsoon

Hyoeun Oh[1], Jong-Ghap Jhun[2], Kyung-Ja Ha[1,3], and Kyong-Hwan Seo[1,3]

[1]*Division of Earth Environmental System, Pusan National University, Busan, Korea*
[2]*School of Earth and Environmental Sciences, Seoul National University, Seoul, Korea*
[3]*Research Center for Climate Sciences, Pusan National University, Busan, Korea*

(Manuscript received 14 October 2016; accepted 10 March 2017)

Abstract: This study investigates the individual effects of the East Atlantic/West Russia (EATL/WRUS) and Western Pacific (WP) teleconnection patterns and their combined effect on the East Asian winter monsoon (EAWM). The contributions of the respective EATL/WRUS and WP teleconnection patterns to the EAWM are revealed by removing the dependence on the Arctic Oscillation (AO) and the El Niño-Southern Oscillation (ENSO) using a linear regression, which are named as N_EATL/WRUS and N_WP, respectively. This is because the EATL/WRUS (WP) is closely linked to the Arctic (tropics) region. A significant increase (decrease) in temperature over East Asia (EA) corresponding to a weak (strong) EAWM is associated with the N_EATL/WRUS and N_WP teleconnection patterns during the positive (negative) phases. In order to examine impacts of these two teleconnections on the EAWM, three types of effects are reconstructed on the basis of ± 0.5 standard deviation: 1) Combined effect, 2) N_EATL/WRUS effect, and 3) N_WP effect. The positive N_EATL/WRUS teleconnection induces to a weakened Siberian High and a shallow EA trough at the mid-troposphere through wave propagation, leading to the weak EAWM. During the positive N_WP pattern, warm air from the tropics flows toward the EA along western flank of an anomalous anticyclone over the North Pacific that is relevant to the meridional shift of the Aleutian Low. When the two mid-latitude teleconnections have the in-phase combination, the increase in temperature over EA appears to be more pronounced than the individual effects by transporting warm air from tropics via strong southeasterly wind anomalies induced by anomalous zonal pressure gradient between the Siberian High and Aleutian Low. Therefore, the impact of the mid-latitude teleconnections on the EAWM becomes robust and linearly superimposed, unlike a nonlinear in-phase combined effect of the AO and ENSO.

Key words: East Asian winter monsoon, East Atlantic/West Russia (EATL/WRUS) teleconnection, Western Pacific (WP) teleconnection, winter temperature

1. Introduction

The East Asian winter monsoon (EAWM) is considered as one of the most energetic circulation systems, and it is affected by tropical-extratropical interactions. The strong (weak) EAWM is relevant to prevailing northerly (southerly) flows induced by an intensified (weakened) Siberian High and Aleutian Low, deep (shallow) East Asia (EA) trough, strong (weak) subtropical jet stream, and the consequent low (high) air temperature over EA (Jhun and Lee, 2004; Ha et al., 2012; Kim et al., 2013; Lee et al., 2013a; Luo and Zhang, 2015). Since abrupt changes in the temperature can exert an influence on the daily lives of people as well as industry and agriculture in this region, it is crucial to fully understand the EAWM even for both social and economic development. It is common knowledge that interannual variability (IAV) of the East Asian monsoon is dependent on many factors such as the El Niño-Southern Oscillation (ENSO) (Wang et al., 2000; Wang et al., 2008; Chu et al., 2012; Chen et al., 2013a; He and Wang, 2013), Arctic Oscillation (AO) (Gong and Ho, 2002; Park et al., 2011; Li et al., 2014; Lim and Kim, 2016), Eurasia (EU) teleconnections (Lim and Kim, 2013; Liu et al., 2014), Western Pacific (WP) pattern (Takaya and Nakamura, 2013; Park and Ahn, 2016), and stratospheric polar vortex (Wei et al., 2016).

Many previous studies have focused on the ENSO and AO as the primary potential predictors of the EAWM variability on interannual timescales. The ENSO is a climate phenomenon that the periodical variation of sea surface temperature (SST) over the tropical eastern Pacific lasts for several months. Wang et al. (2000) proposed that an anomalous anticyclonic circulation at the low-level over the western North Pacific is an essential system that bridges the negative relationship between the EAWM and ENSO, implying that the warming (cooling) phase of ENSO causes a weak (strong) EAWM. Such relationship is weakened from mid-1970 to late-1990 due to climate change (Yun et al., 2008), although it is recovered during the recent decades (Fig. 1; Wang et al., 2008; Wang et al., 2009a; He and Wang, 2013; Lee et al., 2013b; Yang and Wu, 2013; Kim et al., 2014). In contrast, a negative relationship between the EAWM and AO is strengthened after the 1980s due to the reduced Arctic sea ice cover in autumn that modulates jet stream to be extended westward into EA, and it is disrupted during the recent decades (Fig. 1; Li et al., 2014). Thompson and Wallace (2000) have investigated that warm (cold) advection by both anomalous zonal and meridional winds associated with the positive (negative) phase of the AO is responsible for the weak (strong) EAWM and warm (cold)

Corresponding Author: Kyung-Ja Ha, Division of Earth Environmental System, Pusan National University, Busan 46241, Korea.
E-mail: kjha@pusan.ac.kr

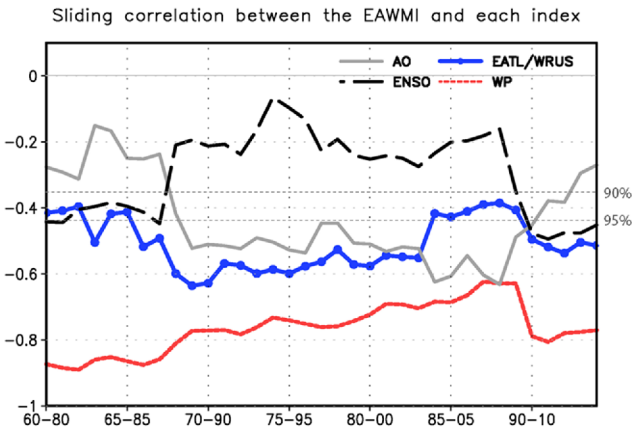

Fig. 1. The 21-yr sliding correlation between the EAWM index and EATL/WRUS, WP, AO, and ENSO. The horizontal dashed lines indicate values significant at the 90% and 95% confidence level.

condition over EA. However, many recent studies suggested that the sole impact of AO does not clearly explain the IAVs of the Siberian High and EAWM activity (Wu et al., 2006; Park et al., 2011; Lim and Kim, 2013; Lim and Kim, 2016). Wu and Wang (2002) demonstrated that the AO and Siberian High are nearly independent in influencing the EAWM activity and cold surge, and the AO accounts for only 13.0% of the Siberian High variation. It remains unclear whether the ENSO and AO are robust factors in affecting the winter climate over EA or not.

The strengths of the Siberian High and Aleutian Low are of great importance for the identification of the EA climate by modulating the intensity of zonal pressure gradient around the EA monsoon region. It suggests that the principal factors to control the pressure variability around EA need to be considered for a better understanding of the variability of the EAWM. The several atmospheric teleconnections during the boreal winter, which classify into north-south dipole and wave train-like patterns, have a close relationship with the EAWM-related circulation pattern (Wallace and Guzler, 1981; Liu et al., 2014). Among the teleconnections, there is a growing interest in impacts of the EU teleconnections, such as conventional EU, Scandinavia, and EATL/WRUS, on the EAWM in the last three decades (Cheung et al., 2012; Lim and Kim, 2013; Liu et al., 2014). The positive phase of the EU teleconnection pattern modulates the EA jet stream to be strengthened, resulting in the cold winter over EA, while that of the EATL/WRUS teleconnection pattern features a zonal wave train-like pattern propagating eastward from the Atlantic to mid-latitude EA with anomalous anticyclone over western Europe and EA, leading to warm winter over EA, and anomalous cyclone over the Atlantic and Siberian region (Barnston and Livezey, 1987; Wang and Zhang, 2015). Since the EU teleconnection pattern is not only somewhat dependent upon the winter mean fields but also its strength is relatively not stationary, we prefer the EATL/WRUS teleconnection pattern to the EU teleconnection pattern (Barnston and Liverzey, 1987; Liu et al., 2014). Lim and Kim (2013) has described that the Siberian High variability has a closer connection with the EATL/WRUS than AO. The condition of the positive (negative) EATL/WRUS phase originating in the North Atlantic weakens (strengthens) the Siberian High intensity and the relevant southeasterly (northwesterly) anomaly over EA (Wang et al., 2011), thereby resulting in warm (cold) conditions over the same region. Thus, the EATL/WRUS teleconnection pattern is more plausible than the AO for explaining the IAV of the Siberian High and EAWM (Wu and Wang, 2002; Lim and Kim, 2013). Some studies have shown that the EAWM is more significantly related to pressure variations of the WP pattern than those of the Aleutian Low (Wang and Chen, 2014; Park and Ahn, 2016). The WP-related circulation has a strong meridional pressure gradient over the North Pacific, which is relevant to the northward shift of the Aleutian Low. The positive (negative) WP pattern is characterized by a dipole pressure structure over the North Pacific and leads to warm (cold) condition over EA and cold (warm) condition over the Okhotsk Sea (Takaya and Nakamura, 2013; Park and Ahn, 2016).

Lim and Kim (2013) has revealed impacts of four dominant teleconnections including AO, EATL/WRUS, WP, and ENSO on the EA winter climate. To clarify the persistent relationships between each index and the EAWM, the 21-yr sliding correlation between the EAWM index and each teleconnection is shown (Fig. 1). The interannual relationship between either the AO or ENSO and EAWM is not stationary, since it includes the conspicuous low-frequency variation (Fig. 1; He and Wang, 2013; Yun et al., 2014). In contrast, the EAWM-WP or EAWM-EATL/WRUS relationship is relatively consistently significant during the whole period at the 90% confidence level. Even though the AO seems significantly correlated with the EAWM during a specific period of 1968-2010, the correlation coefficient between the EAWM and EATL/WRUS teleconnection pattern (0.52) is much higher than that between the EAWM and AO (0.45), which highlights the EAWM-EATL/WRUS relationship. Thus, the present study is motivated by the present limited understanding of the combined effect of the two persistent mid-latitude teleconnections in modulating the EAWM variability.

In the current study, it is shown that key driving forces for the winter monsoon are the EATL/WRUS and WP teleconnection patterns, representing a remote zonal wave-like teleconnection and local north-south dipole pattern, respectively, instead of various high-latitude and tropical effects such as the AO and ENSO which have been mainly studied in the past. Thus, the purpose of the study is to describe the respective effects of the EATL/WRUS and WP teleconnection patterns excluding the AO and ENSO signal, respectively, and their combined effect on the EAWM. In addition, the combined effect of the two mid-latitude teleconnection patterns (EATL/WRUS and WP) would be compared to that of the AO and ENSO. Section 2 displays the observational data and method utilized in this study to exclude the EATL/WRUS and WP

effect from the AO and ENSO, respectively. In section 3, we describe individual climate features associated with the AO-independent EATL/WRUS teleconnection and ENSO-independent WP patterns. Section 4 addresses the impact of the EATL/WRUS and WP teleconnection patterns without the AO and ENSO, respectively, and their combined impact on the EAWM. Finally, the section 5 contains a summary and discussion.

2. Data and method

The monthly atmospheric variables used in this study are derived from the National Centers for Environmental Prediction-National Center for Atmospheric Research (NCEP-NCAR; Kalnay et al., 1996) reanalysis data, which are enough to analyze the classification of patterns. The atmospheric variables are 2 m air temperature (T2m), sea level pressure (SLP), air temperature, zonal wind, meridional wind, and 500 hPa geopotential height. The NCEP-NCAR data have a resolution of 2.5° latitude by 2.5° longitude except for T2m data with a resolution of about 1.9° latitude by 1.9° longitude. The analysis period is the boreal winter from December to February of the following year (DJF) for 55 years from 1960/61 to 2014/15.

Many previous studies have defined the current EAWM indices, including the zonal SLP gradient (Wu and Wang, 2002), low-level meridional wind (Chen et al., 2000; Yang et al., 2002), mid-level EA trough (Wang et al., 2009b), and upper-level horizontal wind shear (Jhun and Lee, 2004; Li and Yang, 2010), as indicators of the intensity of the EAWM. We have selected the EAWM index defined as the deepened EA trough at 500 hPa within 25°-45°N and 110°-145°E, since the index is a suitable for representing the temperature over the EA monsoon region, covering East China, Korea, and Japan (Wang and Chen, 2014). The monthly climate indices (AO, EATL/WRUS, WP, and ENSO [Niño 3.4; 5°S-5°N, 170°-120°W]) are derived from Climate Prediction Center (CPC)-National Oceanic and Atmospheric Administration (NOAA) data (ftp://ftp.cpc.ncep.noaa.gov/wd52dg/data/indices/tele_index.nh).

Since the EAWM has significant interdecadal change around the mid-1980s, all indices are detrended by removing a linear trend. Regression analysis is performed to verify anomalous temperature and atmospheric circulation patterns that are associated with planetary-scale teleconnections. The present study includes the respective contributions of the EATL/WRUS and WP teleconnection patterns to the EAWM without the dependence on the AO and ENSO using a linear regression, respectively (Zhou and Wu, 2010; Wu et al., 2014). The reason of this remove is because the EATL/WRUS and WP teleconnection patterns are closely linked to the AO and ENSO, respectively. In other words, the EATL/WRUS teleconnection pattern has a close relationship with the anomalous cyclone circulation in the high-latitudes, and it exhibits equivalent barotropic structure (figure not shown). Since variations in the AO impact the upper-level westerlies and SLP in the high-latitudes, the dependency of the EATL/WRUS upon the AO might be included. In addition, the WP pattern is shown to influence the occurrence of the ENSO via the stationary wave propagation from the equatorial eastern Pacific to North Pacific (Alexander et al., 2010; Chen et al., 2013a). A linear regression is used to exclude the possible influence dominated by any other teleconnection patterns:

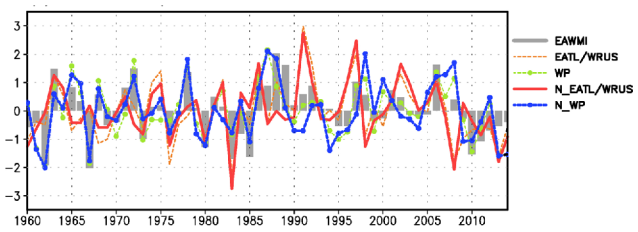

Fig. 2. Normalized time series of the detrended EAWM, EATL/WRUS, WP, N_EATL/WRUS, and N_WP indices in DJF during 1960/61-2014/15.

$$\text{new WP(N\_WP)} = \text{WP} - [r_1\,(\text{WP, ENSO}) \times \text{ENSO}] \quad (1)$$

$$\text{new EATL/WRUS(N\_EATL/WRUS)} = \text{EATL/WRUS} - [r_2\,(\text{EATL/WRUS, AO}) \times \text{AO}] \quad (2)$$

where $r_1(r_2)$ is the regression coefficient of the ENSO (AO) with WP (EATL/WRUS).

Hereafter, the AO-independent EATL/WRUS and ENSO-independent WP pattern are named as new EATL/WRUS (N_EATL/WRUS) and new WP (N_WP), respectively. The correlation coefficient between the N_EATL/WRUS (N_WP) and AO (ENSO) is 0.02 (–0.07) for 55 winters from 1960/61 to 2014/15, representing the N_EATL/WRUS (N_WP) variability is independent with the AO (ENSO). We have categorized into three cases representing the N_EATL/WRUS effect, N_WP effect, and their combined effect and performed composite analysis to explore the associated temperature anomalies and atmospheric circulation for each case.

3. Individual influences associated with the N_EATL/WRUS and N_WP indices

a. Interannual variabilities of the EAWM, N_EATL/WRUS, and N_WP

Figure 2 shows the normalized time series of the detrended EAWM and two types of EATL/WRUS and WP indices during 1960/61-2014/15. The EAWM index, which is defined as the EA trough at 500 hPa over EA, is associated with an intensity of the EAWM and cold surges (Li and Yang, 2010). Positive (negative) EAWM index has a positive (negative) anomaly of geopotential height centered over EA indicating a weakening (strengthening) of the EAWM. The EATL/WRUS and WP teleconnection patterns are related to the EAWM, and the corresponding correlations are highly significant with

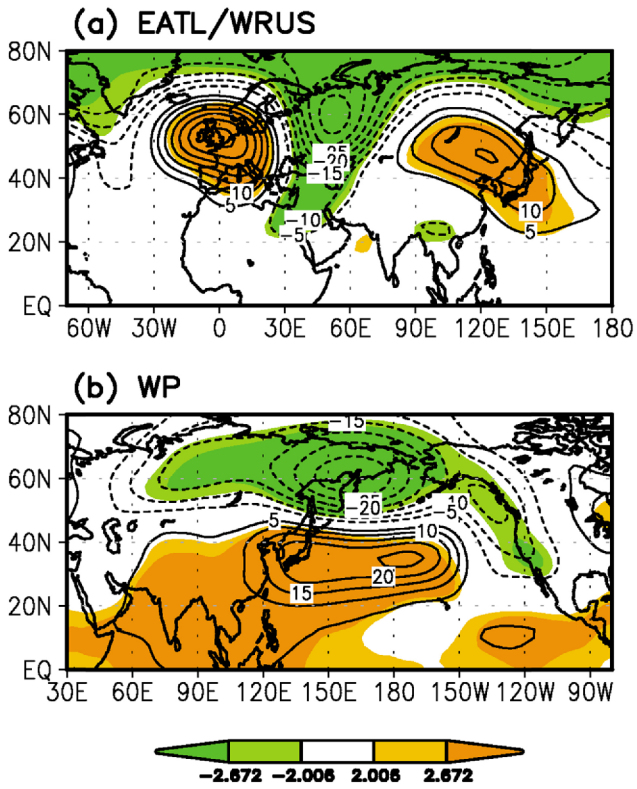

Fig. 3. Regression fields of geopotential height at 500 hPa against (a) EATL/WRUS and (b) WP indices. Light (dark) shading denotes values significant at the 95% (99%) confidence levels.

correlation coefficients of 0.51 and 0.79 above the 99% confidence level, respectively. Moreover, the EATL/WRUS (WP) teleconnection pattern is significantly associated with the AO (ENSO) with a correlation coefficient of 0.41 (0.40), exceeding the 99% confidence level (Horel and Wallace, 1981; Wallace and Gutzler, 1981; Lim, 2015). Figure 3 also displays the regression fields of anomalous 500 hPa geopotential height onto the two mid-latitude teleconnections (EATL/WRUS and WP), regarding to the connection between EATL/WRUS (WP) and AO (ENSO). The EATL/WRUS teleconnection pattern is characterized not only by the wave propagation at the mid-latitudes but also by the atmospheric circulation at the high-latitudes. The zonally symmetric pressure at the high-latitudes appears to be connected to the archetypal AO pattern (Fig. 3a; Thompson and Wallace, 1998). In addition, the WP pattern displays the meridional dipole pressure at the mid-latitudes over the North Pacific, and it is closely linked to the tropics (Fig. 3b).

Now we express that the N_EATL/WRUS (N_WP) teleconnection pattern used is obtained by removing the AO (ENSO) using a linear regression. The correlation between either the N_EATL/WRUS or N_WP and EAWM index shows an obvious drop, with a correlation coefficient of 0.39 and 0.68, respectively. However, the correlation coefficients of the EAWM index with the AO (0.36) and ENSO (0.30) are quite

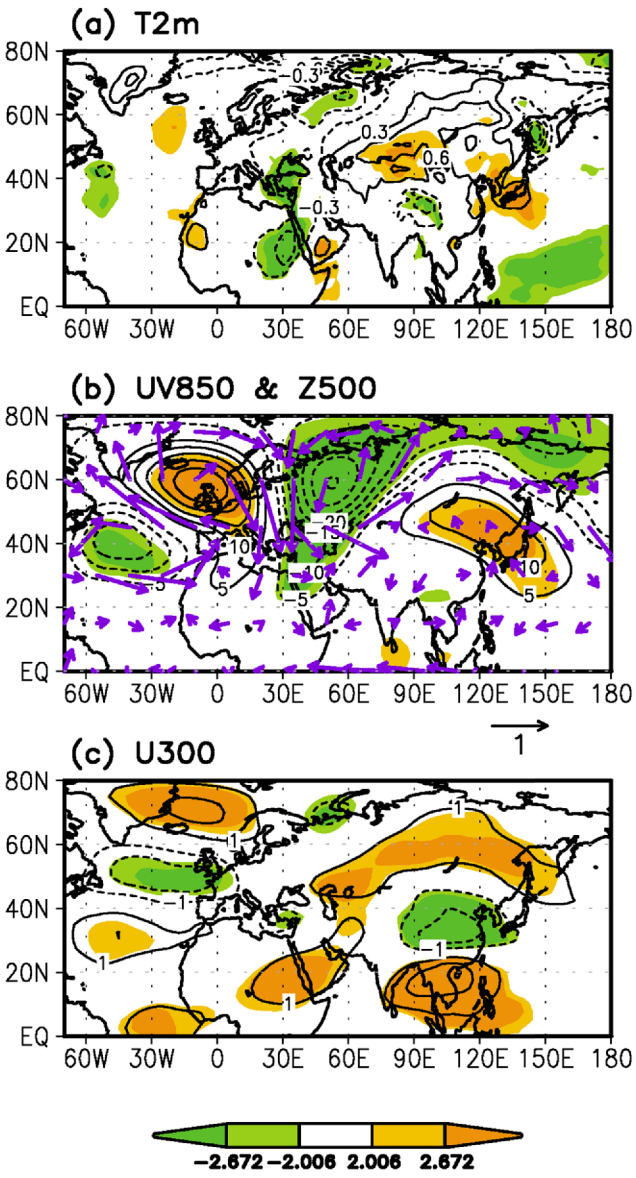

Fig. 4. Regression fields of (a) T2m, (b) low-level wind at 850 hPa (vector) and geopotential height at 500 hPa (contour), and (c) zonal wind at 300 hPa against the N_EATL/WRUS index. Light (dark) shading denotes values significant at the 95% (99%) confidence levels.

lower than those with the N_EATL/WRUS teleconnection and N_WP patterns. It indicates that mid-latitude planetary-scale circulation patterns (EATL/WRUS and WP) have a closer relationship than the high-latitude and tropical processes (AO and ENSO) with the EAWM. We have reviewed NCEP1 data in addition to two other different datasets including the European Centre for Medium-range Weather Forecasts (ECMWF) 40-year reanalysis data (ERA-40; Uppala et al., 2005) and NCEP/Department of Energy AMIP-II reanalysis data set (NCEP-2; Kanamitsu et al., 2002); all exhibit similar variation to each other (figure not shown).

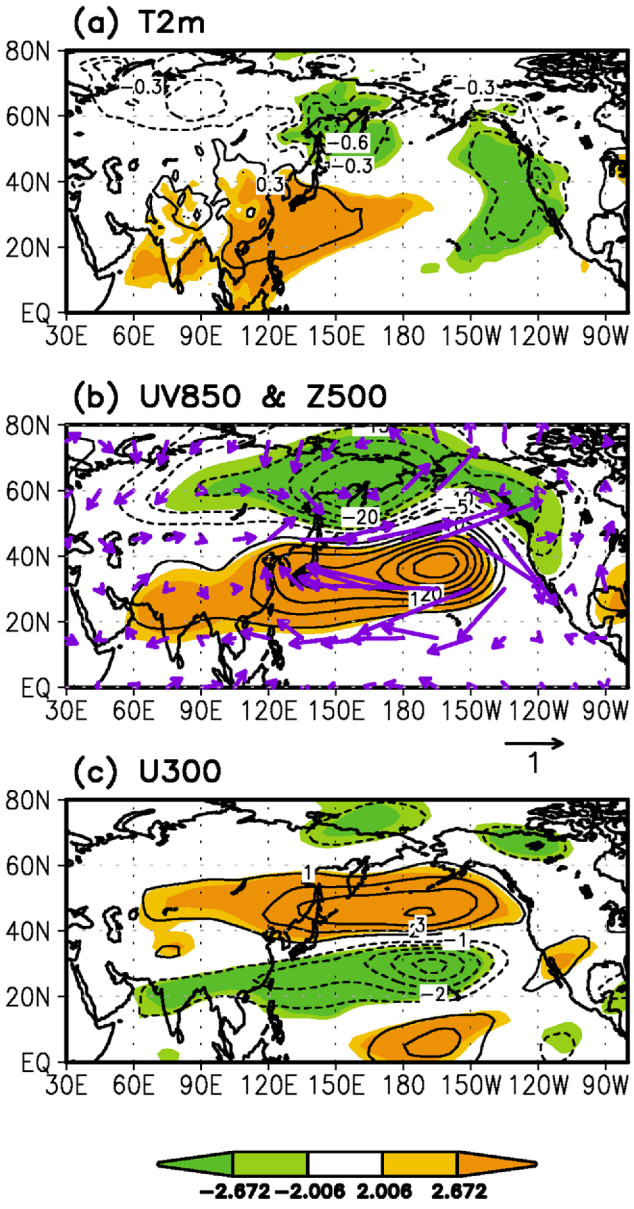

Fig. 5. Same as Fig. 4 but for the N_WP index.

b. Climate features associated with the N_EATL/WRUS and N_WP indices

We address the impact of the N_EATL/WRUS teleconnection and N_WP patterns mainly on their positive phases basis in this paper. The impact is reversed for the negative phase of these teleconnections. In order to better understand atmospheric circulations linked to the N_EATL/WRUS and WP teleconnection patterns, the regressed fields in terms of T2m, 850 hPa low-level wind, 500 hPa geopotential height, and 300 hPa upper-level zonal wind are presented in Figs. 4 and 5. The positive N_EATL/WRUS teleconnection pattern shows that anomalous surface temperature increases over the continental EA near 40°N (Fig. 4a), and it describes an

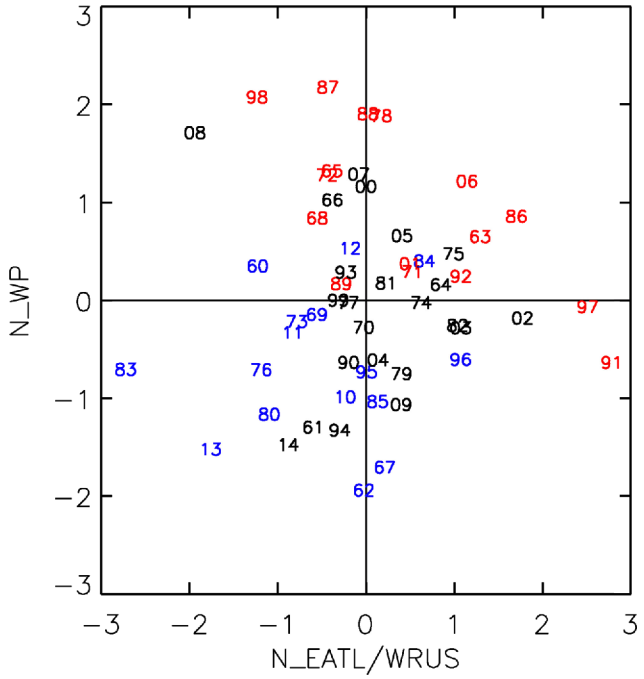

Fig. 6. Scatter diagram between the N_EATL/WRUS and N_WP in DJF. The red (blue) color indicates the weak (strong) EAWM years when the EAWM index is more (less) than 0.5 (−0.5) standard deviation. The numbers denote the indicated years; if the year is 1960/61, it would be shown as '60'.

anomalous cyclone over the Eurasian continent, signifying a weakening of the Siberian High (Lim and Kim, 2013). The weakened atmospheric circulation over the Siberian region can give rise to the positive geopotential height anomaly to the east, driving warm condition over EA via anomalous southerly winds (Fig. 4b). The consequent anomalous southerlies produce a decreased meridional gradient of temperature leading to a weakening of the upper-level jet stream over EA (Fig. 4c). Compared to the original EATL/WRUR teleconnection pattern, the cyclonic circulation anomaly in the high-latitude is weaker but that over the mid-latitude is emphasized, representing that the N_EATL/WRUS teleconnection is well separated from the AO signal. Under the positive condition of the N_WP pattern, the well-established anomalous southeasterly flows at the low-level affect the warming of the T2m south of 40° near EA including the east China, Korea, south Japan, and adjacent marginal seas (Fig. 5a). This results from an atmospheric circulation pattern over the North Pacific, which is relevant to the northward shift of the Aleutian Low (Fig. 5b). In addition, the upper-level jet stream is weakened and migrated northward, thereby resulting in a typical weakened EAWM (Fig. 5c). The northward shift of the upper-level westerlies (Fig. 5c), compared to the climatological location, is physically linked to the enhancement of the meridional dipole structure of pressure anomalies (Figs. 5b and 5c). Also, the anticyclone anomaly is not observed over the tropics any more after removing the ENSO signal (Figs. 3b and 5b).

Table 1. List of years based on the phases of the N_EATL/WRUS and N_WP indices in DJF during 1960/61-2014/15.

years	Combined effect	N_EATL/WRUS effect	N_WP effect
High (Above +0.5σ)	63/64, 86/87, 06/07	64/65, 74/75, 75/76, 82/83, 84/85, 92/93, 97/98, 02/03, 03/04	65/66, 66/67, 72/73, 78/79, 87/88, 88/89, 00/01, 05/06, 07/08
Low (Below −0.5σ)	61/62, 76/77, 80/81, 83/84, 13/14, 14/15	60/61, 69/70, 73/74, 11/12	62/63, 67/68, 79/80, 85/86, 90/91, 94/95, 95/96, 04/05, 09/10, 10/11

4. Impact of the N_EATL/WRUS and N_WP teleconnection patterns and their combined effect on the EAWM

a. Relationship between the N_EATL/WRUS and N_WP

The relationship between the N_EATL/WRUS and N_WP teleconnection patterns is revealed in the scatter plot (Fig. 6). As pointed out before, the correlations of the EAWM index with the N_EATL/WRUS and N_WP teleconnection patterns are significant at the 95% confidence level, and the N_EATL/WRUS index is independent of the N_WP index with the correlation coefficient of 0.03. When the weak (strong) EAWM is obtained based on the criterion of above +0.5σ (below −0.5σ) of the EAWM index, the weak (strong) EAWM usually falls in the first (three) quadrant 1 (3) indicating positively (negatively) in-phase relationship between the N_EATL/WRUS and N_WP teleconnection patterns.

The N_EATL/WRUS and N_WP indices are normalized to be classed as positive (negative) years when the normalized indices are larger (less) than +0.5σ (−0.5σ). In order to compare the individual and combined effects of the N_EATL/WRUS and N_WP teleconnection patterns on the EAWM, we have categorized into three distinct cases based on the criterion of ± 0.5σ: 1) Combined effect; the N_EATL/WRUS and N_WP teleconnection patterns exhibit an in-phase relationship each other. The positively in-phase (1963, 1986, and 2006) and negatively in-phase relationships (1961, 1976, 1980, 1983, 2013, and 2014) between the two mid-latitude teleconnections are selected. 2) N_EATL/WRUS effect; the N_EATL/WRUS is above +0.5σ (1964, 1974, 1975, 1982, 1984, 1992, 1997, 2002, and 2003) or below −0.5σ (1960, 1969, 1973, and 2011) with normal N_WP years to minimize the N_WP effect. 3) N_WP effect; the N_WP is above +0.5σ (1965, 1966, 1972, 1978, 1987, 1988, 2000, 2005, and 2007) or below −0.5σ (1962, 1967, 1979, 1985, 1990, 1994, 1995, 2004, 2009, and 2010) with normal N_EATL/WRUS years to minimize the N_EATL/WRUS effect. All selected years are represented in Table 1. It should be noted that no overlap occurs among three different cases.

b. Respective and combined effect of the N_EATL/WRUS and N_WP

An analysis of a composite difference has been performed to examine the respective and combined impacts of the EATL/WRUS and WP teleconnection patterns on the EAWM. The differences in the composites for above +0.5σ and below −0.5σ years are shown, which are separately conducted by three kinds of effects including (a) Combined effect, (b) N_EATL/WRUS effect, and (c) N_WP effect.

The positive temperature anomalies are shown over the EA monsoon region, while the negative temperature anomalies are found at the high-latitude over the North Pacific except the N_EATL/WRUS effect (Fig. 7). The associated temperature distribution is strongly connected to the north-south pressure dipole anomaly over the North Pacific. The temperature pattern of the N_EATL/WRUS teleconnection is noteworthy over the continental EA. For quantitative changes in temperature over the EA monsoon region, the averaged T2m over the EA monsoon region is estimated. The combined effect (1.26 K) appears to be stronger than the warming by the EATL/WRUS (1.08 K) and WP (0.74 K) alone, and it is nearly the linear combination of each effect. The surface temperature response to the combined effect of the EATL/WRUS and WP teleconnection patterns is compared with that to a combined effect of EATL/WRUS-independent AO (N_AO) and WP-independent ENSO (N_ENSO). When a combined effect of the AO and ENSO is considered without the two mid-latitude teleconnection impacts (EATL/WRUS and WP), the change in temperature over the EA monsoon region is only 0.83 K. Thus, the roles of mid-latitude teleconnection patterns play a crucial role in modulating the winter temperature over EA during the positive in-phase relationship of each other.

We then explore the possible reasons why the combined effect of the N_EATL/WRUS and N_WP teleconnection patterns is more effective in determining the winter temperature over EA. The corresponding circulation patterns such as the SLP, 850 hPa low-level winds, and 300 hPa geopotential height are represented in Fig. 8. The atmospheric circulation patterns associated with the combined effect show the dominant meridional dipole pattern over the North Pacific (i.e., southern anticyclonic and northern cyclonic anomalies along ~50°N) and wave train patterns over the Eurasian continent with a barotropic structure, which are important circulation systems of the EAWM. Since the zonal pressure gradient between the Siberian High and Aleutian Low is reduced, the anomalous southeasterly wind is prominent over EA, thereby inducing the warm winter over the same region (Fig. 8a). The N_EATL/WRUS teleconnection impact on the weakening of

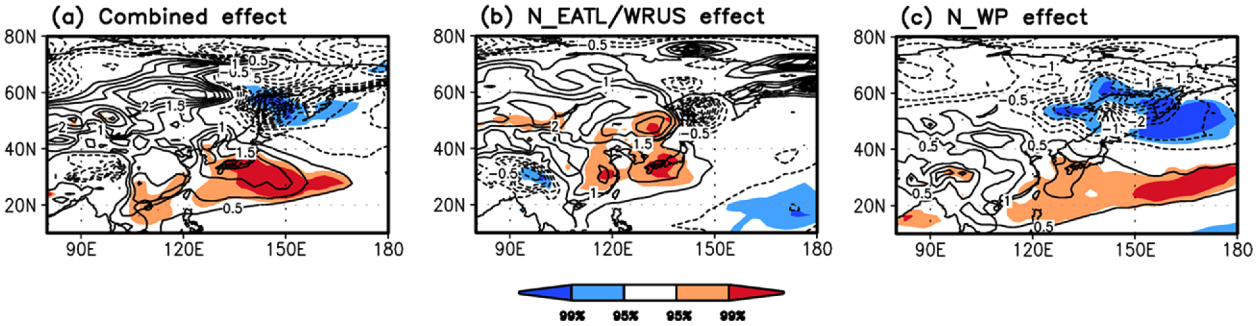

Fig. 7. Composite difference of T2m between high and low years for (a) Combined, (b) N_EATL/WRUS, and (c) N_WP effects. Light (dark) shading denotes values significant at the 95% (99%) confidence levels.

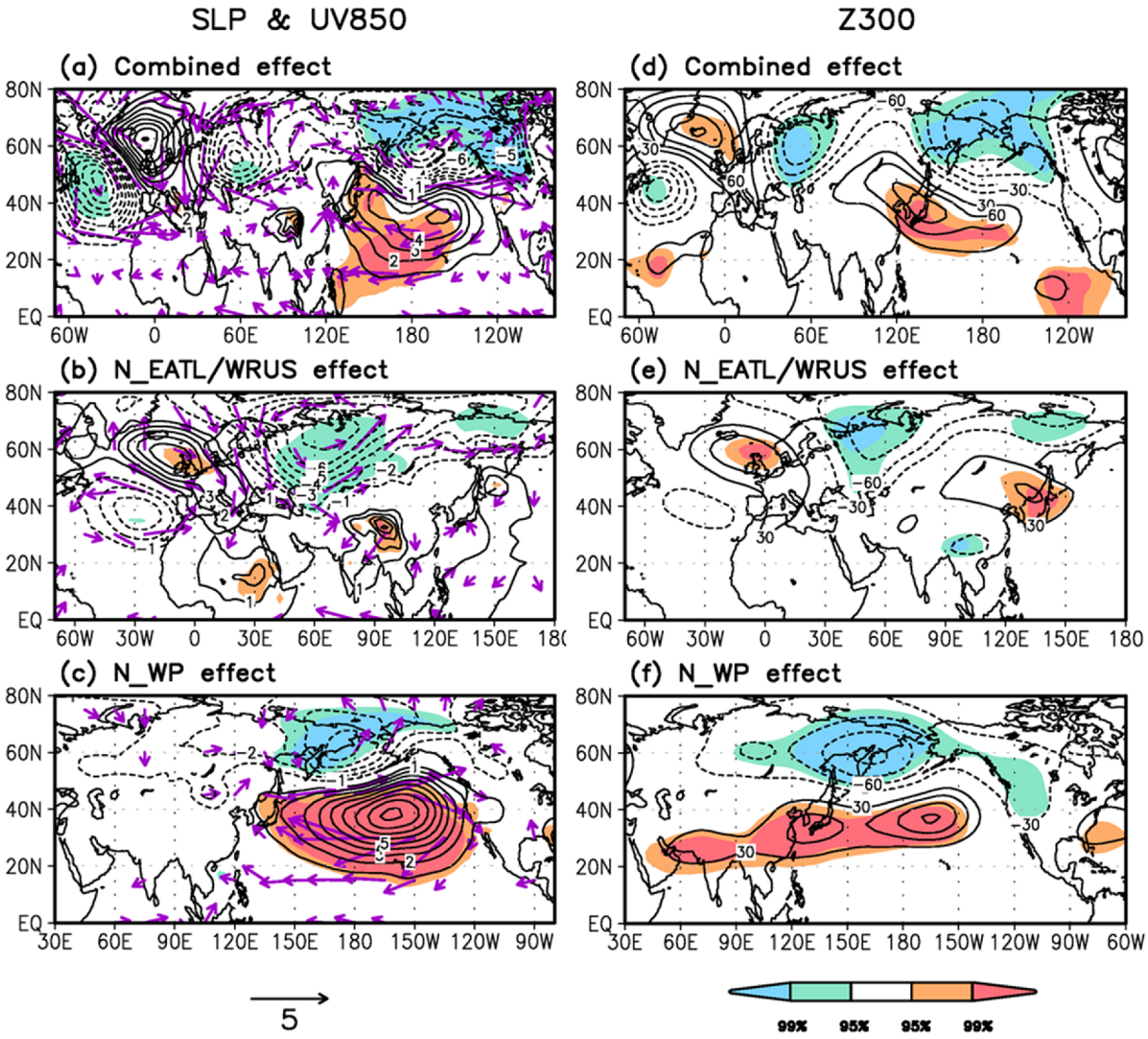

Fig. 8. Same as Fig. 7 but for (a)-(c) SLP (contour) and low-level wind at 850 hPa (above 0.8 m s^{-1}) (vector) and (d)-(f) geopotential height at 300 hPa.

the Siberian High through wave propagation is essential to the warming of surface temperature over EA (Fig. 8b), and its pressure pattern resembles the Ural-Siberian blocking to influence the EA climate (Cheung et al., 2012; Lim and Kim, 2016). In addition, the weakened EA trough at the mid-troposphere, which steers cold temperature from the high

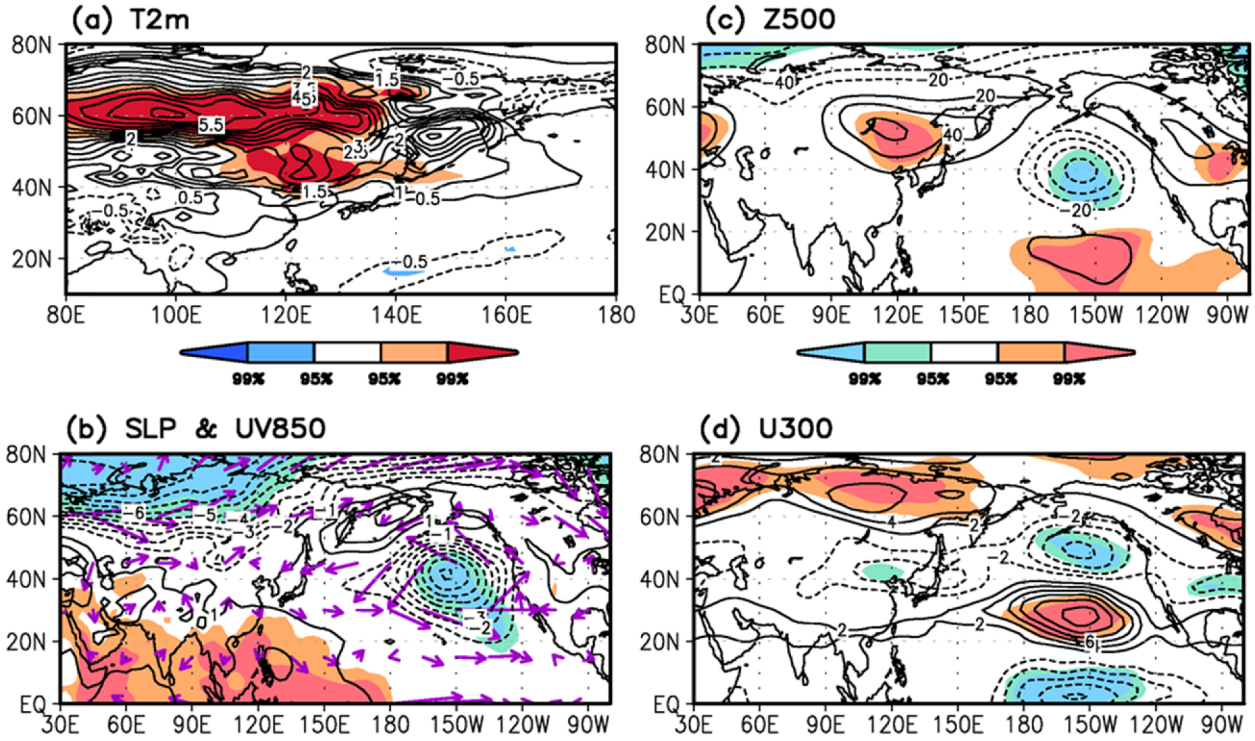

Fig. 9. Composite difference of T2m between high and low years for combined effect of the N_AO and N_ENSO. Light (dark) shading denotes values significant at the 95% (99%) confidence levels.

latitudes to EA, is positioned (Wang et al., 2009b). Since the EA is located on the far eastern side of the EATL/WRUS teleconnection, its impact on low-level circulation over EA could be not established (Fig. 8b; Lim and Kim, 2013). For the positive phase of the N_WP pattern, the weak EAWM would be influenced by the western flank of the anomalous anti-cyclone circulation via anomalous southeasterly flow at the low-level (Figs. 8c and 8f). The corresponding circulation pattern has the strong meridional pressure gradient over the North Pacific that is relevant to the northward shift of the Aleutian Low.

Figure 9 shows the combined effect of the N_AO and N_ENSO without the EATL/WRUS and WP teleconnection patterns, respectively, to compare to that of the two sole mid-latitude teleconnections. There are four years that is positively in-phase relationship between the N_AO and N_ENSO (1972, 1990, 1994, and 2014) and seven years in negatively in-phase relationship between the N_AO and N_ENSO (1964, 1978, 1984, 2000, 2005, 2010, and 2012) for the analysis. The relationship between the EAWM and ENSO is interrupted by atmospheric circulation patterns coupled with the AO, when the in-phase relationship between the AO and ENSO is revealed (Figs. 9b and 9c; Chen et al., 2013b). The combined effect of the N_AO and N_ENSO tends to explain large parts of temperature anomalies for the Eurasia continent, but does not reach the EA region. Specifically, the southern part of China has no significant temperature change, even during El Niño due to strong tropical-extratropical interaction around the EA region (Fig. 9a). A weakening of the upper-level zonal wind corresponds well to the weak EAWM, but its effect has a relatively small. This is contrary to the combined effect of the N_EATL/WRUS and N_WP teleconnection patterns. Thus, the combined effect of two mid-latitude teleconnections can be well explained by a linear superposition of the impacts of the N_EAWL/WRUS and N_WP teleconnection patterns on the EAWM when they have the in-phase relationship, unlike the nonlinear combined effect of the N_ENSO and N_AO.

To further explore the anomalous climate features over EA, the composite difference of the latitude-pressure cross section of zonal wind (Figs. 10a-c) and air temperature (Figs. 10d-f) along 110°-145°E are shown for the three different effects. Corresponding to the weak EAWM characteristics, the centers of upper-level westerly jet are shifted northward (Figs. 10a-c). The upper-level westerlies shifted northward is physically linked to enhanced meridional dipole structure of the pressure and temperature anomalies with thermal wind relationship (Fig. 10c; Linkin and Nigam, 2008). In addition, some previous studies have mentioned that the opposite surface temperature signals between the north and south EA region are associated with the strength of the stratospheric polar vortex by modulating the upper level jet via wave-mean flow interaction (Fig. 7c; Wang et al., 2010; Wei et al., 2016). The significant increase of temperature exists over the EA monsoon region below the 500 hPa, thereby resulting in the weakening of the EAWM (Figs. 10d-f). The temperature increase over EA is associated with not only the weak jet stream at the upper-level

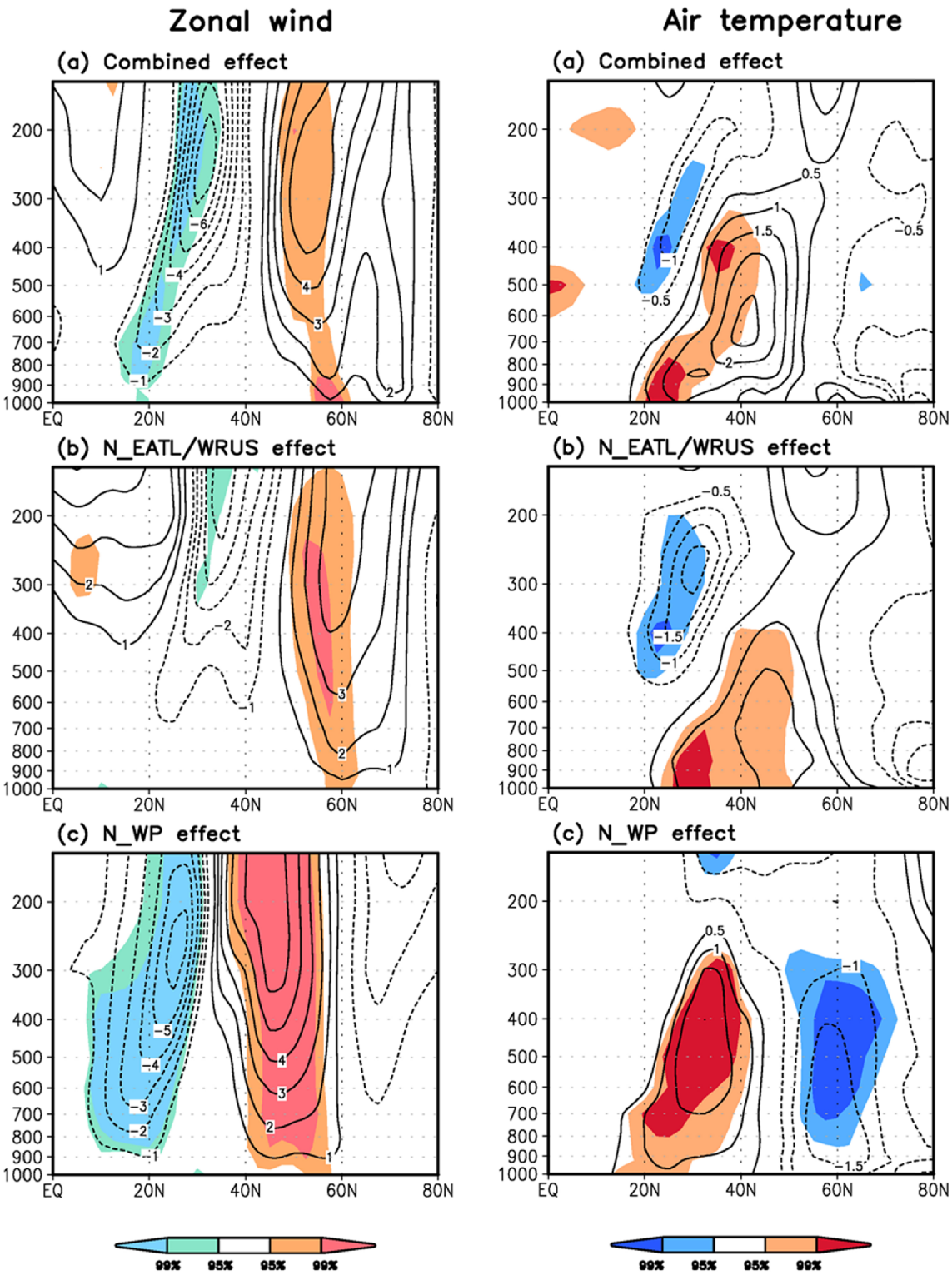

Fig. 10. Composite difference of latitude-level cross section of (a)-(c) zonal wind, (d)-(f) air temperature between high and low years for (a) and (d) Combined, (b) and (e) N_EATL/WRUS, and (c) and (f) N_WP effects. Light (dark) shading denotes values significant at the 95% (99%) confidence levels.

but also a strong southerly flow at the low-level that transports warm air from the tropics. It indicates that the anomalous southeasterly toward EA may bring about anomalous warm advection (Fig. 11). A horizontal thermal advection is more substantial than the other thermodynamic terms (figure not shown). The anomalous warm advection is noted along the

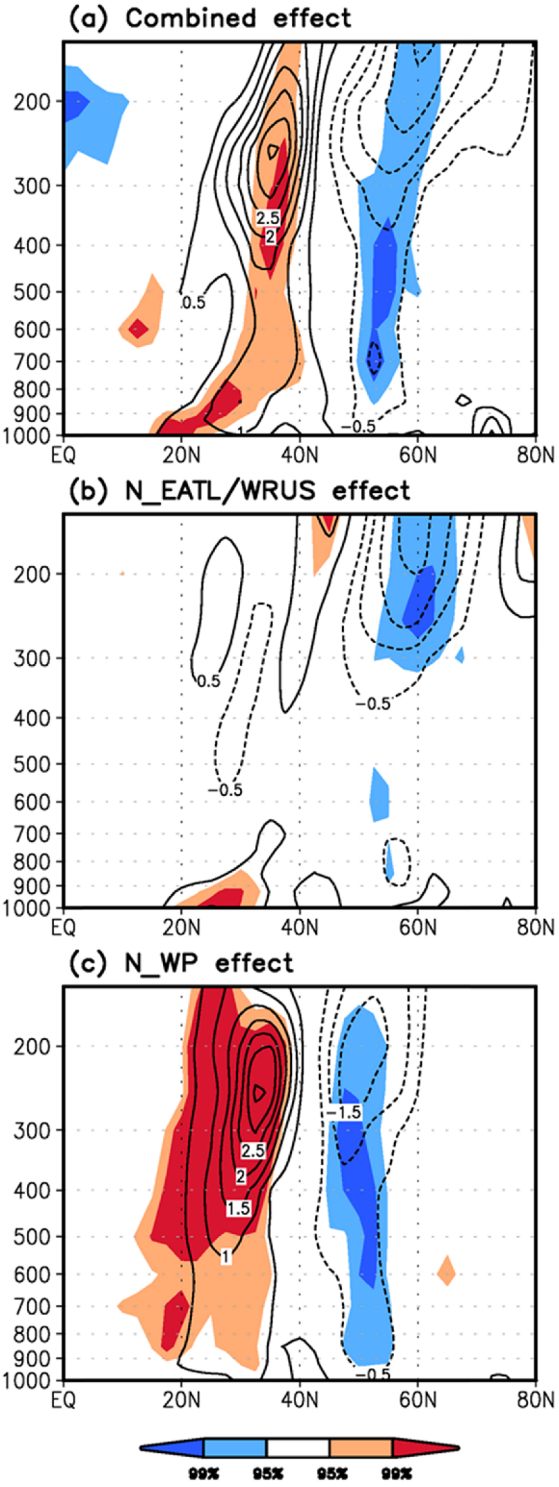

Fig. 11. Same as Fig. 10 but for thermal advection (contour interval is 1×10^5).

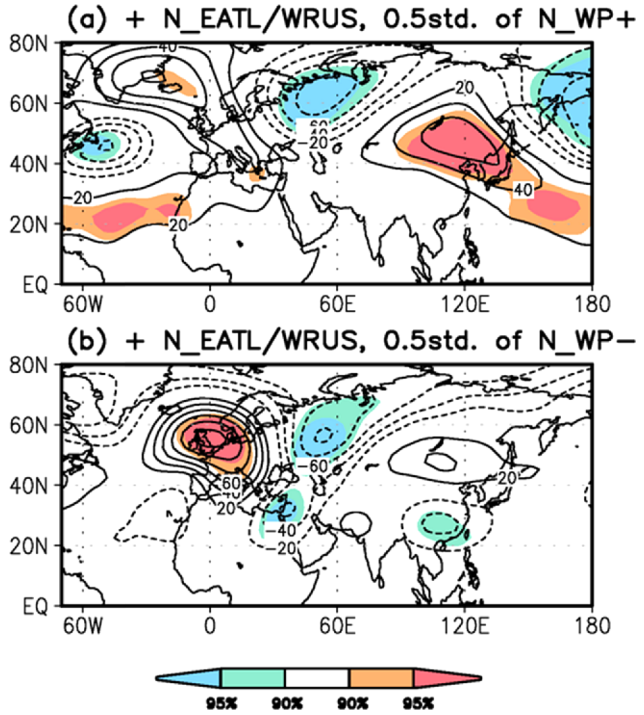

Fig. 12. Composite maps of the geopotential height at 300 hPa for the cases of (a) positive N_EATL/WRUS and positive N_WP teleconnection patterns (in-phase) and (b) positive N_EATL/WRUS and negative N_WP teleconnection patterns (out-of-phase). Light (dark) shading denotes values significant at the 95% (99%) confidence levels.

western flank of positive pressure anomaly over the North Pacific by the prevailing anomalous southeasterly, with a barotropic structure under the positive N_WP pattern (Figs. 8 and 11). On the contrary, the zonal temperature advection associated with easterly flow from the positive circulation anomaly over the North Pacific contributes predominantly to the positive thermal advection anomalies of the combined effect (figure not shown). The thermal advection associated with the N_EATL/WRUS teleconnection across the Eurasian continent is a relatively weakened at the low-level, since the EA is located at the far eastern side of the downstream region of the teleconnection (Figs. 9 and 10b).

5. Summary and discussion

The impact of the mid-latitude teleconnections (EATL/WRUS and WP) on the EAWM has less attention compared to that of the high-latitude and tropical processes. However, the influence of the mid-latitude teleconnections has been persistent, and it could remarkably contribute to the EA climate variation. Through the 21-yr sliding correlation between the EAWM and each teleconnection pattern including AO, ENSO, EATL/WRUS, and WP, we have revealed that the EAWM-EATL/WRUS or EAWM-WP relationship is consistently robust during 1960/61-2014/15. Moreover, the correlation coefficient between the EAWM and EATL/WRUS (0.52) has been much higher than that between the EAWM and AO (0.45). Regarding to the relationship between the EAWM and WP, the correlation coefficient is 0.79, which is statistically significant at the 99% confidence level. It is enough to

highlight the importance of the EATL/WRUS and WP teleconnection pattern. Since the EATL/WRUS (WP) teleconnection pattern is significantly associated with the AO (ENSO) with a correlation coefficient of 0.41 (0.40), exceeding the 99% confidence level, we have removed the dependent factors to elucidate the respective effects of the AO-independent EATL/WRUS and ENSO-independent WP based on a linear regression. In other words, the N_EATL/WRUS and N_WP indices have been obtained by removing the AO and ENSO, respectively, which correlations with the EAWM are still significant with correlation coefficients of 0.39 and 0.68 at the 95% confidence level. Meanwhile, the N_EATL/WRUS teleconnection pattern is independent from the N_WP pattern with a correlation coefficient of 0.03.

In order to investigate the respective and combined impacts of the EATL/WRUS and WP teleconnection patterns on winter temperature and circulation over EA without the AO and ENSO effect, respectively, we have divided the effects into three groups: 1) Combined effect, i.e., combined effects of positive (negative) N_EATL/WRUS years and positive (negative) N_WP years, 2) N_EATL/WRUS effect, i.e., positive (negative) N_EATL/WRUS years with normal N_WP years, and 3) N_WP effect, i.e., positive (negative) N_WP years with normal N_EATL/WRUS years. The atmospheric circulation associated with the combined effect show the dominant meridional dipole structure over the North Pacific (i.e., southern anticyclonic and northern cyclonic anomalies along ~50°N) and wave train patterns over the Eurasian continent with a barotropic structure, which are important circulation systems of the EAWM. Both the circulation patterns appear to be strongly connected to warm horizontal advection by easterly flow along the anomalous anticyclone over the North Pacific. The positive N_EATL/WRUS teleconnection impact on the weakening of the Siberian High through eastward wave propagation from the Atlantic to mid-latitude EA is essential to the warming of surface temperature over the EA. The N_EATL/WRUS teleconnection pattern mostly have an influence on the significant change in the zonal pressure gradient by weakening of the Siberian High, resulting in the increase in temperature anomaly of the north part of EA during its positive phase. For the positive N_WP phase, the meridional dipole patterns over the North Pacific are significant. The corresponding upper-level jet stream migrates northward, and the Aleutian Low is also shifted to north. These two spatial distributions of these patterns at the mid-latitudes are quite close to the regressed patterns associated with the weak EAWM on the interannual time scale.

The influence of the combined N_EATL/WRUS and N_WP teleconnection patterns on the EAWM nearly shows linear combination effects of each factor. When the combined N_EATL/WRUS and N_WP has the in-phase relationship, the winter atmospheric circulation is more intensified than individual effects of each other. Since variations of the N_WP pattern impact the upper-level westerlies over the North Pacific, the response of the EATL/WRUS teleconnection pattern would be different depending on the N_WP phase (Fig. 12). During the positive N_WP phase (in-phase with the N_EATL/WRUS), the eastward propagation of the N_EATL/WRUS teleconnection is stronger than the negative N_WP phase (out-of-phase with the N_EATL/WRUS) due to the change in strength of the upper-level westerlies. Thus, the N_EATL/WRUS teleconnection is strongly affected by the phases of the N_WP pattern. On the contrary, Chen et al. (2013b) have represented that the combined effect of the N_AO and N_ENSO shows the nonlinear combination effects and cancels each other out. Regarding to the interdecadal variation of the relationships among the EAWM and four distinct indices, Wang et al. (2013) have attributed the enhanced (weakened) relationship between the AO and EAWM to the weakened (enhanced) relationship between the ENSO and EAWM. However, the physical processes in terms of the unstable relationships are still insufficient, and what is more possible causes on consistent linkages between the WP (EATL/WRUS) teleconnection and EAWM variability sustained are not fully discovered in this study. Therefore, further studies should be needed to discover the physical mechanisms to maintain the EAWM-EATL/WRUS or EAWM-WP relationship during the whole analysis periods.

Acknowledgements. This work was supported by the National Research Foundation of Korea (NRF) grant funded by the Korea government (MEST) (No.2011-0021927, GRL) H. Oh was supported by NRF-2015R1C1A1A01054992.

Edited by: Akio Kitoh

References

Alexander, M. A., D. J. Vimont, P. Chang, and J. D. Scott, 2010: The impact of extratropical atmospheric variability on ENSO: Testing the seasonal footprinting mechanism using coupled model experiments. *J. Climate*, **23**, 2885-2901, doi:10.1175/2010JCLI3205.1.

Barnston, A. G., and R. E. Livezey, 1987: Classification, seasonality and persistence of low-frequency atmospheric circulation pattern. *Mon. Wea. Rev.*, **115**, 1093-1126, doi:10.1175/1520-0493(1987)115<1083:CSAPOL>2.0.CO;2.

Chen, W., H.-F. Graf, and R.-H. Huang, 2000: The interannual variability of East Asian winter monsoon and its relation to the summer monsoon. *Adv. Atmos. Sci.*, **17**, 48-60, doi:10.1007/s00376-000-0042-5.

_____, J. Feng, and R. Wu, 2013a: Roles of ENSO and PDO in the link of the East Asian winter monsoon to the following summer monsoon. *J. Climate*, **26**, 622-635, doi:10.1175/JCLI-D-12-00021.1.

_____, X. Q. Lan, L. Wang, and Y. Ma, 2013b: The combined effects of the ENSO and the Arctic Oscillation on the winter climate anomalies in East Asia. *Chinese Sci. Bull.*, **58**, 1355-1362, doi:10.1007/s11434-012-5654-5.

Chu, J.-E., N. H. Saji, K.-J. Ha, 2012: Nonlinear, intraseasonal phases of the East Asian summer monsoon: Extraction and analysis using selforganizing maps. *J. Climate*, **25**, 6975-6988, doi:10.1175/JCLI-D-11-00512.1.

Cheung, H. N., W. Zhou, H. Y. Mok, and M. C. Wu, 2012: Relationship between Ural-Siberian blocking and the East Asian winter monsoon in relation to the Arctic Oscillation and the El Niño-Southern Oscillation. *J. Climate*, **25**, 4242-4257, doi:10.1175/JCLI-D-11-00225.1.

Gong, D.-Y., and C.-H. Ho, 2002: The Siberian high and climate change

over middle to high latitude Asia. *Theor. Appl. Climatol*., **72**, 1-9, doi: 10.1007/s007040200008.

Ha, K.-J., K.-Y. Heo, S.-S. Lee, K.-S. Yun, and J.-G. Jhun, 2012: Variability in the East Asian monsoon: A review. *Meteor. Appl.*, **19**, 200-215, doi:10.1002/met.1320.

He, S., and H. Wang, 2013: Oscillating Relationship between the East Asian winter monsoon and ENSO. *J. Climate.*, **26**, 9819-9838, doi: 10.1175/JCLI-D-13-00174.1.

Horel, J. D., and J. M. Wallace, 1981: Planetary-scale atmospheric phenomena associated with the Southern Oscillation. *Mon. Wea. Rev.*, **109**, 813-829, doi:10.1175/1520-0493(1981)109<0813:PSAPAW>2.0.CO;2.

Jhun, J.-G., and E.-J. Lee, 2004: A new East Asian winter monsoon index and associated characteristics of winter monsoon. *J. Climate*, **17**, 711-726, doi:10.1175/1520-0442(2004)017<0711:ANEAWM>2.0.CO;2.

Kalnay, E., and Coauthors, 1996: The NCEP/NCAR 40-year reanalysis project. *Bull. Amer. Meteor. Soc.*, **77**, 437-471, doi:10.1175/1520-0477(1996)077<0437:TNYRP>2.0.CO;2.

Kanamitsu, M., W. Ebisuzaki, J. Woollen, S.-K. Yang, J. J. Hnilo, M. Fiorino, and G. L. Potter, 2002: NCEP-DOE AMIP-II reanalysis (R-2). *Bull. Amer. Meteor. Soc.*, **83**, 1631-1643, doi:10.1175/BAMS-83-11-1631.

Kim, J.-W., S.-W. Yeh, and E.-C. Chang, 2014: Combined effect of El Nino-Southern oscillation and Pacific decadal oscillation on the East Asian winter monsoon. *Climate Dyn.,* **42**, 957-971, doi:10.1007/s00382-013-1730-z.

Kim, Y., K.-Y. Kim, and J.-G. Jhun, 2013: Seasonal evolution mechanism of the East Asian winter monsoon and its interannual variability. *Climate Dyn.*, **41**, 1213-1228, doi:10.1007/s00382-012-1491-0.

Lee, J.-Y., S.-S. Lee, B. Wang, K.-J. Ha, and J.-G. Jhun, 2013a: Seasonal prediction and predictability of the Asian winter temperature variability. *Climate Dyn.*, **41**, 573-587, doi:10.1007/s00382-012-1588-5.

Lee, S.-S., S.-H. Kim, J.-G. Jhun, K.-J. Ha, and Y.-W. Seo, 2013b: Robust warming over East Asia during the boreal winter monsoon and its possible causes. *Environ. Res. Lett*., **8**, 034001, doi:10.1088/1748-9326/8/3/034001.

Li, F., H. J. Wang, and Y. Q. Gao, 2014: On the strengthened relationship between East Asian winter monsoon and Arctic oscillation: A comparison of 1950-1970 and 1983-2012. *J. Climate*, **27**, 5075-5091, doi:10.1175/JCLI-13-00335.1.

Li, Y., and S. Yang, 2010: A dynamical index for the East Asian winter monsoon. *J. Climate*, **23**, 4255-4262, doi:10.1175/2010JCLI3375.1.

Lim, Y.-K., and H.-D. Kim, 2013: Impact of the dominant large-scale teleconnections on winter temperature variability over East Asia. *J. Geophys. Res.*, **118**, 7835-7848, doi:10.1002/jgrd.50462.

_____, 2015: The East Atlantic/West Russia (EA/WR) teleconnection in the North Atlantic: Climate impact and relation to Rossby wave propagation. *Climate Dyn.*, **44**, 3211-3222, doi:10.1007/s00382-014-2381-4.

_____, and H.-D. Kim, 2016: Comparison of the impact of the Arctic oscillation and Eurasian teleconnection on interannual variation in East Asian winter temperatures and monsoon. *Theor. Appl. Climatol.,* **124**, 267-179, doi:10.1007/s00704-015-1418-x.

Linkin, M. E., and S. Nigam, 2008: The North Pacific oscillation-West Pacific teleconnection pattern: Mature-phase structure and winter impacts. *J. Climate*, **21**, 1979-1997, doi:10.1175/2007JCLI2048.1.

Liu, Y. Y., L. Wang, W. Zhou, and W. Chen, 2014: Three Eurasian teleconnection patterns: Spatial structures, temporal variability, and associated winter climate anomalies. *Climate Dyn.*, **42**, 2817-2839, doi:10.1007/s00382-014-2163-z.

Luo, X., and, Y. A. Zhang, 2015: The linkage between upper-level jet streams over East Asia and East Asian winter monsoon variability. *J. Climate*, **28**, 9013-9028, doi:10.1175/JCLI-D-15-0160.1.

Park, H.-J., and J.-B. Ahn, 2016: Combined effect of the Arctic oscillation and the Western Pacific pattern on East Asia winter temperature. *Climate Dyn.*, **46**, 3205-3221, doi:10.1007/s00382-015-2763-2.

Park, T.-W., C.-H. Ho, and S. Yang, 2011: Relationship between the Arctic oscillation and cold surges over East Asia. *J. Climate*, **24**, 68-83, doi:10.1175/2010JCLI3529.1.

Takaya, K., and H. Nakamura, 2013: Interannual variability of the East Asian winter monsoon and associated modulations of the planetary waves. *J. Climate*, **26**, 9445-9461, doi:10.1175/JCLI-D-12-00842.1.

Thompson, D. W. J., and J. M. Wallace, 1998: The Arctic oscillation signature in the wintertime geopotential height and temperature fields. *Geophys. Res. Lett*., **25**, 1297-1300. doi:10.1029/98GL00950.

_____, and _____, 2000: Annular modes in the extratropical circulation. Part I: Month-to-month variability. *J. Climate*, **13**, 1000-1016, doi: 10.1175/1520-0442(2000)013<1000:AMITEC>2.0.CO;2.

Uppala, S. M., and Coauthors, 2005: The ERA-40 re-analysis. *Quart. J. Roy. Meteor. Soc.*, **131**, 2961-3012, doi:10.1256/qj.04.176.

Wallace, J. M., and D. S. Gutzler, 1981: Teleconnections in the geopotential height field during the Northern Hemisphere winter. *Mon. Wea. Rev.*, **109**, 784-812, doi:10.1175/1520-0493(1981)109<0784:TITGHF>2.0.CO;2.

Wang, B., R. Wu, and X. Fu, 2000: Pacific-East Asian teleconnection: How does ENSO affect East Asian climate? *J. Climate*, **13**, 1517-1536, doi:10.1175/1520-0442(2000)013<1517:PEATHD>2.0.CO;2.

_____, Z. Wu, C.-P. Chang, J. Liu, J. Li, and T. Zhou, 2010: Another look at interannual-to-interdecadal variations of the East Asian winter monsoon: The Northern and Southern temperature modes. *J. Climate*, **23**, 1495-1512, doi:10.1175/2009JCLI3243.1.

Wang, H., S. He, and J. Liu, 2013: Present and future relationship between the East Asian winter monsoon and ENSO: Results of CMIP5. *J. Geophys. Res*., **118**, 5222-5237, doi:10.1002/jgrc.20332.

Wang, L., and W. Chen, 2014: An intensity index for the East Asian winter monsoon. *J. Climate*, **27**, 2361-2374, doi:10.1175/JCLI-D-13-00086.1.

_____, W. Chen, and R. H. Huang, 2008: Interdecadal modulation of PDO on the impact of ENSO on the East Asian winter monsoon. *Geophys. Res. Lett.*, **35**, L20702, doi:10.1029/2008GL035287.

_____, R. Huang, L. Gu, W. Chen, and L. Kang, 2009a: Interdecadal variations of the East Asian winter monsoon and their association with quasi-stationary planetary wave activity. *J. Climate*, **22**, 4860-4872, doi:10.1175/2009JCLI2973.1.

_____, W. Chen, W. Zhou, and R. H. Huang, 2009b: Interannual variations of East Asian trough axis at 500 hPa and its association with the East Asian winter monsoon pathway. *J. Climate*, **22**, 600-614, doi:10.1175/2008JCLI2295.1.

Wang, N., and Y. Zhang, 2015: Evolution of Eurasian teleconnection pattern and its relationship to climate anomalies in China. *Climate Dyn.*, **44**, 1017-1028, doi:10.1007/s00382-014-2171-z.

Wang, X., C. Wang, W. Zhou, D. Wang, and J. Song, 2011: Teleconnected influence of North Atlantic sea surface temperature on the El Niño onset. *Climate Dyn.*, **37**, 663-676, doi:10.1007/s00382-010-0833-z.

Wei, K., Z. Cai, W. Chen, and L. Xu, 2016: The effect of a well-resolved stratosphere on East Asian winter climate. *Climate Dyn.*, doi:10.1007/s00382-016-3419-6.

Wu, B., and J. Wang, 2002: Winter Arctic oscillation, Siberian high and East Asian winter monsoon. *Geophys. Res. Lett.*, **29**, 1897, doi:10.1029/2002GL015373.

_____, R. Zhang, and R. D'Arrigo, 2006: Distinct modes of the East Asian winter monsoon. *Mon. Wea. Rev.*, **134**, 2165-2179, doi:10.1175/MWR3150.1.

Wu, R., W. Chen, G. Wang, and K. Hu, 2014: Relative contribution of ENSO and East Asian winter monsoon to the South China Sea SST anomalies during ENSO decaying years. *J. Geophys. Res. Atmos*., **119**, 5046-5064, doi:10.1002/2013JD021095.

Yang, L. N., and B. Y. Wu, 2013: Interdecadal variations of the East Asian winter surface air temperature and possible causes. *Chinese Sci. Bull*., **58**, 3969-3977, doi:10.1007/s11434-013-5911-2.

Yang, S., K. M. Lau, and K. M. Kim, 2002: Variations of the East Asian jet stream and Asian-Pacific-American winter climate anomalies. *J. Climate*, **15**, 306-325, doi:10.1175/1520-0442(2002)015<0306:VOTEAJ>2.0.CO;2.

Yun, K.-S., S.-H. Shin, K.-J. Ha, A. Kitoh, and S. Kusunoki, 2008: East Asian Precipitation Change in the Global Warming Climate Simulated by a 20-km Mesh AGCM, Asia-Pac. *J. Atmos. Sci*., **44**, 233-247.

_____, Y.-W. Seo, K.-J. Ha, J.-Y. Lee, and Y. Kajikawa, 2014: Interdecadal changes in the Asian winter monsoon variability and its relationship with ENSO and AO. *Asia-Pac. J. Atmos. Sci.*, **50**, 531-540, doi:10.1007/s13143-014-0042-5.

Zhou, L.-T., and R. Wu, 2010: Respective impacts of the East Asian winter monsoon and ENSO on winter rainfall in China. *J. Geophys. Res.*, **115**, D02107, doi:10.1029/2009JD012502.